Design of Circularly Polarized Modified Minkowski Fractal Based Antenna for UHF RFID Reader Applications

Shashi Kant Pandey [1,2], Ganga Prasad Pandey [3], and P. M. Sarun[1]

[1]Department of Applied Physics, Indian Institute of Technology (ISM), Dhanbad, Jharkhand, India - 826004
[2]Department of Applied Physics, Maharaja Agrasen Institute of Technology, Delhi, India -110086
[3]Department of ICT, Pandit Deendayal Petroleum University, Gandhinagar, Gujarat, India
*corresponding author, E-mail: ganga.mait@gmail.com

Abstract

A compact, square shaped microstrip fractal antenna with asymmetrical pairs of T-slits for circularly polarized (CP) radiation and radio frequency identification (RFID) reader applications is proposed and experimentally investigated. Design is based on narrow slit modified Minkowski island fractal geometry. Circular polarization along with size reduction is achieved by inserting four symmetrical pairs of T-slits at the square patch boundary of the single-probe-feed radiator. Proposed geometry is tuned at resonant frequency of 914 MHz by optimization of dimensions of the two T-slits. Compactness of the antenna is achieved by increasing the overall sizes of the slits. Antenna is fabricated on FR4 substrate with a size of $47.2\times47.2\times1.6$ mm^3 ($0.143\lambda_0 \times 0.143\lambda_0 \times 0.005\lambda_0$) and tested to validate the simulated results. The 3-dB axial-ratio (AR) bandwidth and impedance bandwidth of the proposed antenna design are found to be 7 MHz (911-918 MHz) and 24 MHz (909-933 MHz) respectively. A design equation is develped based on the parametric study that can be used to design a compact antenna with CP for UHF RFID applications covering the frequency range from 887 to 1023 MHz.

Index Terms- Axial-ratio bandwidth, Circular polarization, Minkowski fractal, RFID reader, Microstrip antenna**.**

1. Introduction

RFID is a versatile technology that passed through many decades of use in military, airlines, library, healthcare management, animal farms, supermarkets and shops for inventory management, patrolling and many other applications. Recently compact, handheld RFID system in the ultra high frequency (UHF, 850-950 MHz) band has gained popularity in many applications such as logistics, supply chain management and automatic toll collection system as it provides highest readable range (3-6 meters in passive and more than 30 meters in active tags [1] and faster reading speed [2]. The RFID system consists of a reader and a tag. RFID reader antennas collect data from tags and therefore, used as a medium for tag reading. Usually, the UHF tag antennas are linearly polarized while tags (objects) containing codes are randomly oriented arising polarization loss consequently lowered signal strength. Therefore circularly polarized antenna for the RFID readers has become ideal candidate to get efficient UHF RFID system. Circularly polarized microstrip antennas (CPMSAs) can effectively control the losses occurred due to multipath effects between tag and reader. Low frequency (LF,30-500 kHz) and high frequency (HF, 10-15 MHz) RFID tags are license exempted and can be used worldwide, whereas UHF RFID require permit and frequency range is different in different region of the world: 902–928 MHz in America , 865–867 MHz in Europe and 840–955 MHz in Asia-Pacific region. Further in Asia-Pacific region, the UHF RFID frequency range is sub-divided country-wise: India (865–867 MHz), China (840.5–844.5 MHz, 920.5–924.5 MHz), Japan (952–955 MHz), Australia (920–926 MHz), Taiwan (920–928 MHz), Korea (908.5–910 MHz, 910–914 MHz), etc. In [3], [4], broadband CPMAs are reported, which cover complete frequency band of the UHF for RFID applications. These designs were very bulky and not suitable for portable/handheld reader applications.

In UHF RFID, commonly two types of circularly polarized (CP) antennas are used. First stacked CPMSA [5-10] and second, single layer single feed microstrip CP antennas [11]–[15]. In [5], a stacked annular-ring patch CP antenna is proposed for UHF RFID band. It provides larger impedance bandwidth at the cost of large and bulky antenna size. In [6], stacked circular patch with slot is proposed to produce CP from 901-930 MHz by using a L shaped probe feed. In [7], a cross-shaped slot and a microstrip strip patch proximity coupled with ground plane are used to produce CP radiation in the UHF range. In [8], many meandered monopole elements fed by a series feed network are proposed for generating CP radiation in the UHF band. These antennas are not suitable for handheld/portable reader applications. The major consideration for CPMA design of handheld/portable RFID application is the compact size of antenna with considerable/moderate impedance bandwidth, AR Bandwidth (ARBW) and gain. Therefore MSA with CP and small size need to be designed for portable RFID system with low specific absorption ratio (SAR). Small size CPMSA can be designed with single layer single feed technique. These antennas have several other advantages

over the stacked CPMAs such as light weight, low cost, easy to fabricate etc. A multilayer dual feed CP antenna was proposed in [9]. The antenna provides high gain due to parasitic patch and air substrate. The feed structure is complex and need physical support for robustness. A broadband CP square ring antenna with multiple feeds is presented in [10. The structure consists of Wilkinson power divider to feed the patch at two orthogonal points to obtain CP. In [11], single feed configuration based asymmetric circular shaped slotted square microstrip patch has been proposed to get the compact size and CP radiations. The authors in [12] presented optimized design of CPMSA using single feed and compactness with CP was achieved with the help of cross slot in [13]. The antenna was made more compact in [14] using arrowhead shaped slot on the patch. In the recent literatures several techniques have been reported to produce CP polarization accompanied with the size reduction of antennas [12-15].

Recently, idea of fractal geometries has been adopted for multiband, wideband and compact microstrip antennas [16-18] design. In [16], size reduction and CP radiations were achieved by placing two asymmetric Koch fractal geometries on horizontal and vertical edges of the single probe feed square patch and ARBW ranging from 907-915 MHz was achieved while fine tuning of bands is achieved by inserting four arrow shaped slots. However, deign is very complex in nature. In[17], asymmetrical Koch fractal curved boundaries with 45^0 tilted scaled fractal slot at centre of radiating patch is used to create tri-band CP radiation at operating frequencies around 2.45 GHz, 3.4 GHz, and 5.8 GHz respectively. In [18], CP operation is achieved by introducing two pairs of symmetrical T-slits at the boundary of a square patch microstrip antenna around 1930 MHz. In addition, approximately 34.3% of size reduction in the antenna, compared to conventional size CP antenna without slits, is obtained. However the size of antenna is still not suitable for handheld UHF FRID reader applications. Table 1 shows the comparison of the performance parameters of the proposed design with the other antennas which are recently reported in the literatures for UHF RFID application. The dimension is calculated at centre frequency of 3-dB ARBW.

In this paper, a compact CPMSA using Modified Minkowski fractal (MMF) geometry for handheld UHF RFID reader application is proposed. The reference antenna is chosen to be a square patch in order to excite two orthogonal modes with close resonant frequencies required for circular polarization. Two T-shaped slots of different dimensions are introduced along the edges of the square patch to make the resonant frequency differ by small amount. Symmetrical fractals are cut on the opposite edges and asymmetric fractal cuts on the adjacent edges of the reference structure. Sizes of the fractal T's are used to tune up the antenna for minimum AR, AR bandwidth, wide impedance bandwidth, and size reduction around 914 MHz. The CP performance of proposed antenna is simulated in detail using IE3D commercial electromagnetic simulator [19] and results are validated with the measured values.

Table 1: Comparison of performance parameters of the proposed antenna with other UHF RFID antennas with CP

S.N.	Ref.	Dimension	Impedance BW(MHz)	ARBW (MHz)
1	[4]	$0.463\lambda_0\times0.463\lambda_0\times0.104\lambda_0$	760 - 963	818 - 964
2	[6]	$0.458\lambda_0\times0.458\lambda_0\times0.103\lambda_0$	880 - 1100	901 - 930
3	[5]	$0.675\lambda_0\times0.675\lambda_0\times0.04\lambda_0$	870 - 967	893 - 948
4	[3]	$0.455\lambda_0\times0.455\lambda_0\times0.06\lambda_0$	800 - 980	820 - 1000
5	[7]	$0.184\lambda_0\times0.184\lambda_0\times0.046\lambda_0$	909 - 937	917 - 929
6	[11]	$0.277\lambda_0\times0.277\lambda_0\times0.015\lambda_0$	904 - 941	918 - 929
7	[13]	$0.276\lambda_0\times0.276\lambda_0\times0.015\lambda_0$	904 - 922	908 - 914
8	[14]	$0.26\lambda_0\times0.26\lambda_0\times0.015\lambda_0$	888 - 923	908 - 916
9	[8]	$0.137\lambda_0\times0.137\lambda_0\times0.027\lambda_0$	912 - 927	906 - 921
10	[15]	$0.185\lambda_0\times0.185\lambda_0\times0.005\lambda_0$	877 -987	914 - 937
11	[16]	$0.164\lambda_0\times0.164\lambda_0\times0.005\lambda_0$	891 - 928	907 - 915
12	**Proposed**	$\mathbf{0.143\lambda_0\times0.143\lambda_0\times0.005\lambda_0}$	**909 - 933**	**911 - 918**

2. Fractal geometry and Antenna design

Minkowski island fractal is well known and its geometry is generated in an iterative fashion that provides self similar structures. In addition to the conventional Minkowski fractal, narrow slit (narrow pulse) models have been proposed and discussed in [20-22]. In [23], narrow slit fractal technique is used to design L-band CP antenna, in which length-width ratio of slits are larger than 5. In [18], a modified Minkowski fractal (MMF) based geometry, having a square microstrip fractal antenna is proposed for achieving CP operation around 1930 MHz. In the design of proposed antenna, asymmetrical dual T-shaped MMF (second order iteration) is implemented to get CP radiation at a relatively lower band of frequency. The top and side view of the proposed T–shaped MMF antenna is shown in Fig.1.

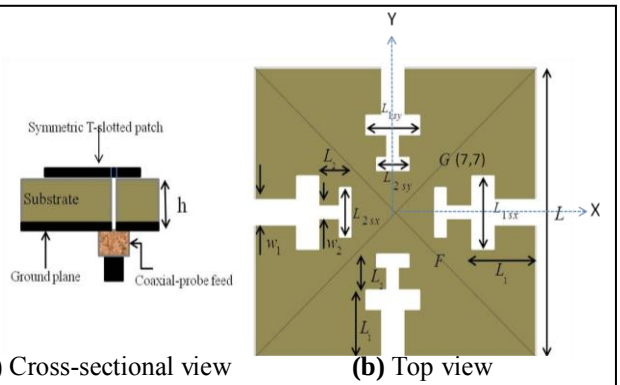

(a) Cross-sectional view **(b)** Top view

Figure1: Schematic of the proposed CP microstrip antenna

The compact antenna of dimension 47.2 mm× 47.2 mm× 1.6 mm is designed and fabricated on low cost FR4 substrate of relative permittivity (ε_r) 4.4 and loss tangent 0.02, suitable for portable/handheld UHF RFID reader application. Height (L_1) and width (W_1) of horizontal as well as vertical T's are same whereas the lengths of the cap of horizontal and vertical T's are L_{1sx} and L_{1sy} respectively. Similarly four inner T-slits, characterized by L_2, L_{2sx}, L_{2sy} and W_2, are scaled versions of corresponding outer slits as shown in Fig.1 (b).The evolution process of proposed antenna geometry involves three steps as pictured in Fig.2;

Step1: Square patch (Antenna A) is designed and fed at the appropriate point along the diagonal. This can excite two orthogonal modes TM_{10} and TM_{01} along horizontal and vertical edge of the patch respectively, without any phase difference. This is 0^{th} iteration or mother structure.

Step2: For CP operation, phase quadrature between two orthogonal modes is introduced by perturbing the sides of the patch with the help of T-slit of dimension given in Table 2 (Antenna B). This may be considered as 1^{st} iteration of the proposed fractal geometry.

Step3: For size reduction and frequency tuning of the antenna, further two pairs of the T- slits of unequal dimensions are introduced internally and connected with the external T-slits (Antenna C). The internal T-slits are scaled down version (with scale factor, δ=0.63 %) of the outer T's. This is 2^{nd} iteration and proposed fractal geometry. The Proposed antenna of desired impedance BW and ARBW are obtained by optimization of IF. A structural dimension of the proposed antenna is summarized in Table 2.

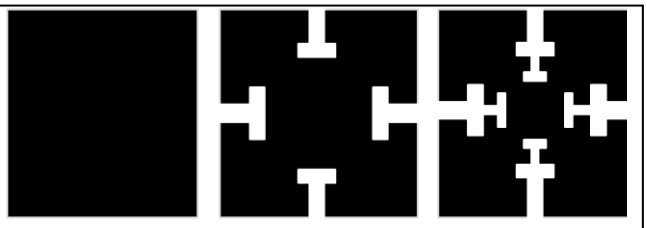

(a) Antenna A **(b)** Antenna B **(c)** Antenna C

Figure 2: Different stages of antenna evolution

Table 2: Geometrical parameters of the proposed antenna (all in mm)

Parameters	**L**	**L_{1sx}**	**L_{1sy}**	**L_1**	**W_1**
Value	47.2	11.304	7.976	9.42	1.57
Parameters	**W_2**	**L_{2sx}**	**L_{2sy}**	**L_2**	
Value	0.63*W_1	0.63*L_{1sx}	0.63*L_{1sy}	0.63*L_1	

3. Symmetrical modified Minkowski fractal structures and simulation Results

In this paper, all the presented results are obtained by taking 'F' as excitation point. A simple square patch (antenna A) of dimension 47.2 mm× 47.2 mm as shown in Fig 2(a) is fed coaxially. Here minimum value of axial ratio is found to be 34.75 dB at 1500 MHz. Such large AR proved the presence of linearly polarized radiation instead of CP, negating the advantage of circular polarization as discussed in the introduction, failing to be good condition for RFID reader application. In antenna B, two pairs of T-shaped slots were cut at the boundary of the square patch as shown in Fig. 2(b) to create two orthogonal modes of equal amplitudes and 90^0 phase difference. The good CP (minimum axial ratio AR = 0.40 dB) radiation is achieved around resonance frequency 1184 MHz. Antenna B was further improved by inserting another two pairs of fractal T- slots as shown in Fig 2(c), namely antenna C. CP operation in UHF FRID tag reader frequency range is achieved by optimization of the sizes of internal T-slots. 3-dB ARBW and impedance BW for antenna B and antenna C are found to be 7 MHz (911-918 MHz) and 24 MHz (909-933 MHz), respectively. To visualize the sense of CP radiation of the proposed antenna, simulated surface current distributions on the patch for four phase angles 0^0 (time t = 0), 90^0 (t = T/4), 180^0 (t = T/2) and 270^0 (t = 3T/4) at 914 MHz is depicted in Fig. 3(a)-(d). Arrows show the direction of currents with the change in phase angle by 90^0. Left hand circular polarization (LHCP) operation is achieved at feed point 'F', whereas right hand circular polarization (RHCP) operation is achieved by changing the feed location to other diagonal position 'G'.

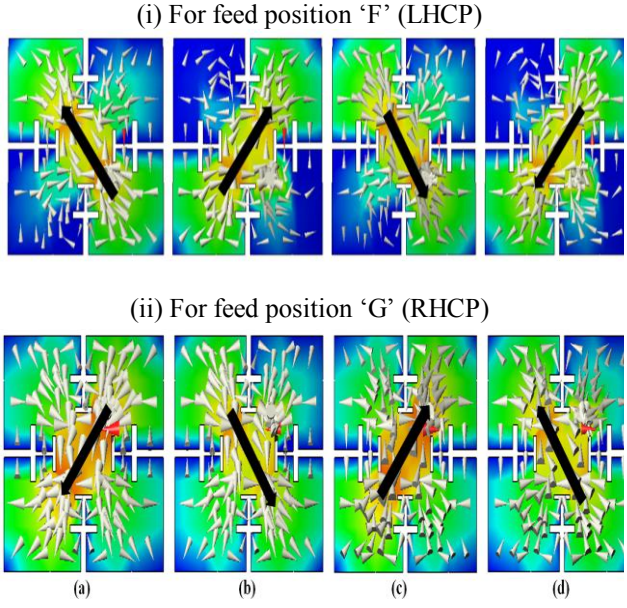

Figure 3: Simulated surface current distributions on the patch of proposed antenna at 914 MHz for different time phases: (a) 0^0 (b) 90^0 (c) 180^0 and (d) 270^0

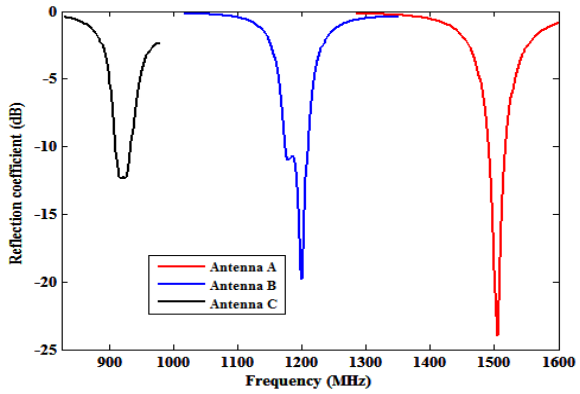

Figure 4: Simulated reflection coefficient variation with frequency for various antennas

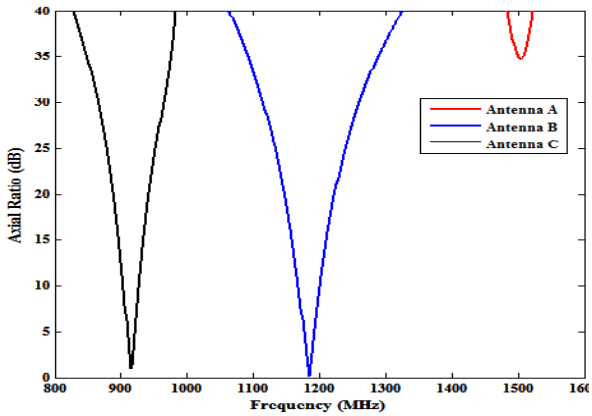

Figure 5: Simulated axial ratio (AR) variation with frequency for various antennas

The simulated reflection coefficient characteristics of the proposed antenna at different stages of evolutions are plotted in Fig.4. Figure illustrates that the resonance frequencies are continuously shifted downwards (1502 MHz for antenna A to 920 MHz for antenna C) due to increase in the electrical length of vector current. In this way, a patch area reduction of 40.2% for the antenna C (proposed) compared to earlier reported compactness [14] using same substrate. Figure 5 depicts the axial ratio (AR) against frequency in the broadside direction ($\theta = 0^0$) for all antennas. No CP band is obtained in the antenna geometry A, whereas antennas B and C provide ARBW of 10 MHz (1178-1188 MHz) and 7 MHz (911-918 MHz) with central frequencies 1184 and 914 MHz having minimum AR of 0.40 and 1.0 dB respectively. Figure 5 shows the shifting of AR center frequency towards the lower side of frequency spectrum with the evolution of design. It is also noticeable that both the reflection coefficient and AR dip at the same frequency.

4. Parametric studies and numerical modeling

Parametric studies are very helpful to engineers for antenna designing and its optimization. The antenna performance to achieve good CP in the desired frequency range (902-928 MHz) is studied by varying the size of internal T's with respect to the external. This parameter, named as scale factor δ (ratio of corresponding dimension of internal and external T's) is independently varied by keeping all other parameters unchanged. Fig.6 illustrates the effect of scale factor δ on the reflection coefficient. It is observed that with increasing δ, the resonance frequency is shifted towards the lower value whereas impedance bandwidth remains unchanged.

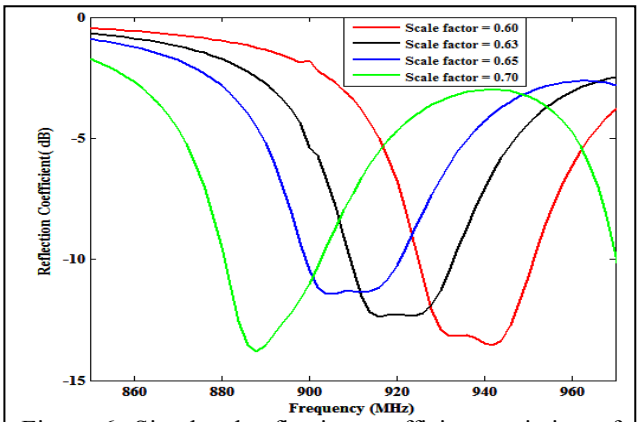

Figure 6: Simulated reflection coefficient variation of the proposed antenna with frequency for various δ

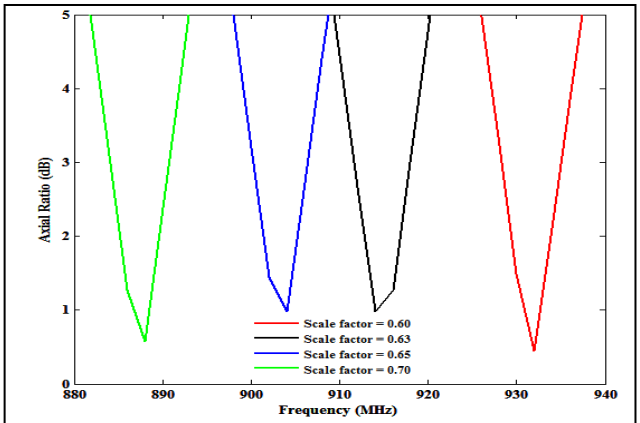

Figure 7: Simulated axial ratio variation of the proposed antenna with frequency for various δ

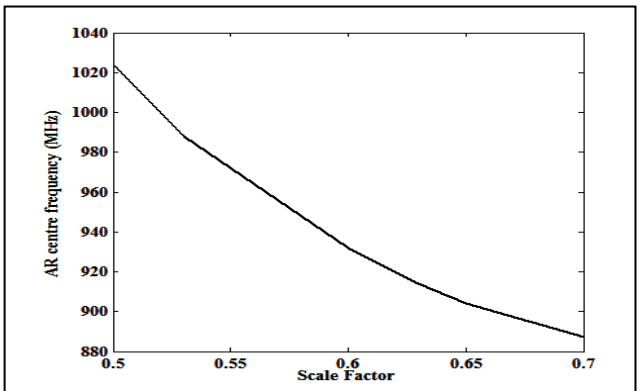

Figure 8: Variations of AR centre frequency with scale factor δ

A similar effect was seen on the axial ratio performance of proposed antenna with frequency for different values of δ and is shown in Fig.7. No significant effect of variation of δ on the axial ratio bandwidth (ARBW) is observed. On the other hand, δ is an efficient tool for adjusting the band of CP operation. This effect was further explained by plotting Fig 8, which demonstrates the variation of AR centre frequency with δ. The effect of δ on various antenna parameters is shown in Table 3. The proposed design provides CP for the value of δ ranging from 0.5 to 0.7 with center frequency of CP band ranging from 1024 MHz to 887MHz. The required scale factor δ for CP center frequency f_d (in GHz) is given by equation (1),

$$\delta = \frac{3.5 - \sqrt{(9.36 f_d - 8.15)}}{4.68}, \qquad (1)$$

This equation has been established on the basis of parametric study of antenna.

Table 3: Parametric study of various antenna parameters with δ

Scale factor (δ)	Resonance frequency (MHz)	Impedance Bandwidth (MHz)	AR centre frequency (MHz)	ARBW (MHz)
0.50	1023	1009-1038	1024	1021-1027
0.53	989	978-1001	988	985-990
0.60	933	924-950	932	928-935
0.63	920	909-933	914	911-918
0.65	904	900-920	904	900-906
0.7	887	880-902	887	883-890

5. Experimental results and discussion

Proposed antenna was fabricated and design parameters were measured to validate the simulated results by using Agilent N5230A vector network analyzer and anechoic chamber. Fig. 9 shows the simulated and measured reflection coefficient with frequency. Measured Impedance bandwidth for reflection coefficient less than -10 dB is 18 MHz (from 911 to 929 MHz). Fig.10 exhibits the simulated and measured AR at the bore sight. Measured value of 3-dB ARBW is 7 MHz (from 911 to 918 MHz) around centre frequency 915 MHz. Results show that ARBW falls within the impedance bandwidth of the proposed antenna, which satisfy the requirement of RFID reader application.

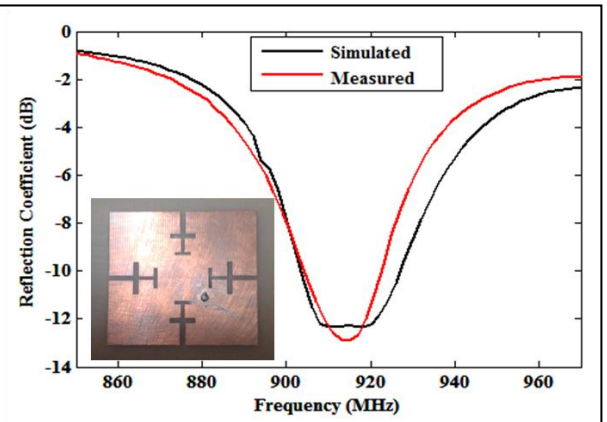

Figure 9: Measured and simulated reflection coefficient of proposed MM fractal based microstrip antenna

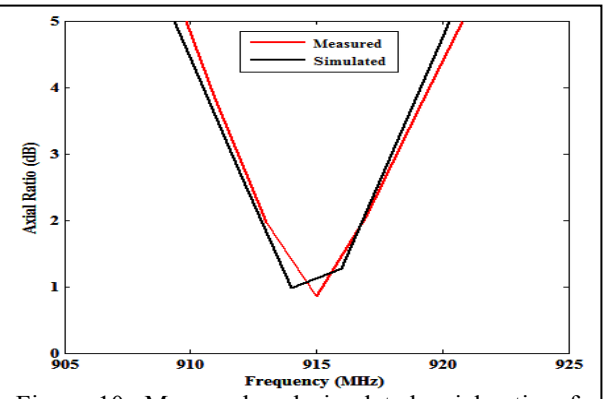

Figure 10: Measured and simulated axial ratio of proposed antenna

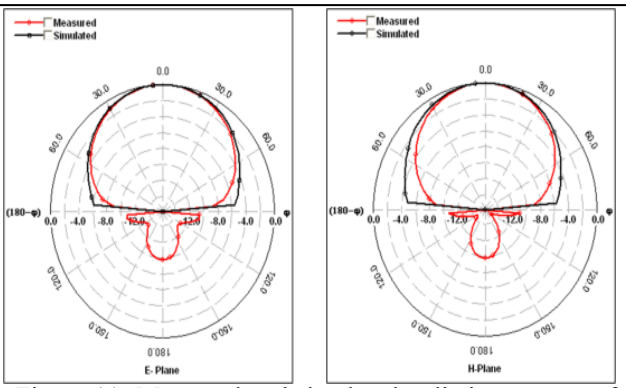

Figure 11: Measured and simulated radiation pattern of proposed MM fractal based CP microstrip antenna at 914 MHz (a) *x-z* plane (E-plane), (b) *y-z* plane (H-plane).

Fig. 11 shows the measured and simulated radiation pattern of the proposed antenna at 914 MHz in two orthogonal planes x-z and y-z. The simulated and measured results of proposed antenna match within acceptable limit. The simulated and measured AR variation with angle in the two orthogonal planes x-z and y-z at centre frequency of 914

MHz are plotted in Fig.12, which shows symmetry about broadside direction and wide CP beamwidth in both x-z and y-z planes. From Figure 12, it is also clear that AR shows symmetry in both x-z and y-z planes. The measured AR beam width in E-plane is 100^0 and H-plane is 115^0 respectively. Fig. 13 shows variation of gain of proposed antenna with frequency at bore sight. The antenna exhibits moderate peak gain of 3.8 dBic (simulated) at 914 MHz. A small difference in simulated and measured gain is due to fabrication and measuring errors. Gain at the bore sight is smaller than what obtained in [16] because of the compact structure of the proposed antenna.

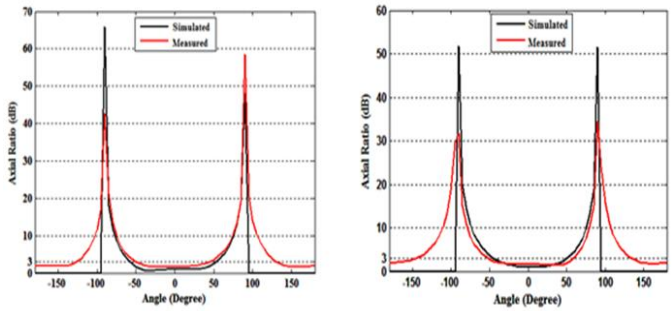

Figure 12: Variation of Simulated AR with angle of the proposed CP antenna at 914 MHz for feed location 'F'. (a) *x-z* plane, (b) *y-z* plane

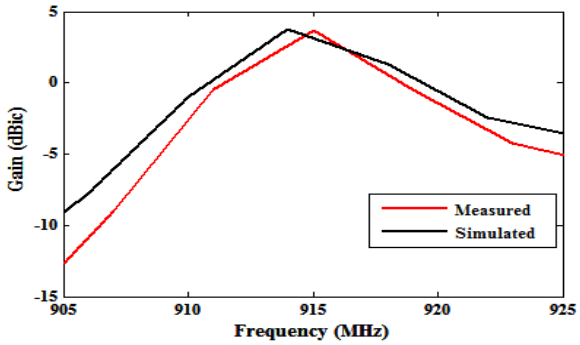

Figure 13: Measured and simulated peak gain of proposed MM fractal based microstrip antenna

6. Conclusions

A compact modified Minkowski fractal based circularly polarized antenna with symmetrical two pairs of T-slits fed by a probe has been presented for handheld UHF RFID applications. Size reduction, band shifting and optimization of other antenna parameters have been done by optimizing the scale factor of the fractal geometry. The proposed antenna design exhibit an axial ratio bandwidth of 7 MHz (911-918 MHz) and impedance bandwidth of 24 MHz (909-933 MHz). Both LHCP and RHCP radiation can be achieved by changing the feed location from one diagonal to other diagonal of the square patch of the proposed structure. The antenna can be deigned to work at different UHF bands by using the design equation developed in the paper. Also the antenna exhibits symmetrical and good AR beam width in space.

References

[1] K. Ahshan, H. Shah and P. Kingston, "RFID applications: an introductory and exploratory study," *IJCSI International Journal of Computer Science Issues*, Vol. 7, Issue 1(3), January 2010.

[2] C.-D. Kim, K. Finkenzeller, *RFID Handbook*, 2nd ed. New York: Wiley, 2003.

[3] H. L. Chung, X. Qing, and Z. N. Chen, "Broadband circularly polarized stacked probe-fed patch antenna for UHF RFID applications," *Int. J. Antennas Propag.*, vol. 2007, pp. 1–9, 2007.

[4] Z. N. Chen, X. Qing, and H. L. Chung, "A universal UHF RFID reader antenna," *IEEE Trans Microwave Theory Tech.*, vol. 57, no. 5, pp. 1275–1282, May 2009.

[5] X. Chen, G. Fu, S.-X. Gong, Y.-L. Yan, and W. Zhao, "Circularly polarized stacked annular-ring microstrip antenna with integrated feeding network for UHF RFID readers," *IEEE Antennas Wireless Propag. Lett.*, vol. 9, 2010.

[6] C.-Y.-D. Sim and C.-J. Chi, "A slot loaded circularly polarized patch antenna for UHF RFID reader," *IEEE Trans. Antennas Propag.*, vol. 60, no. 10, pp. 4516–4521, Oct. 2012.

[7] Y.-F. Lin, C.-H. Lee, S.-C. Pan, and H.-M. Chen, "Proximity-fed circularly polarized slotted patch antenna for RFID handheld reader," *IEEE Trans. Antennas Propag.*, vol. 61, no. 10, pp. 5283–5286, Oct. 2013.

[8] J.-H. Bang, C. Bat-Ochir, H.-S. Koh, E.-J. Cha, and B.-C. Ahn, "A small and lightweight antenna for handheld RFID reader applications", *IEEE Antennas Wireless Propag. Lett.*, vol. 11, 2012.

[9] X. Zhau, Y. Huang, J. Li, Q. Zhang and G. Wen, "Wideband high gain circularly polarised UHF RFID reader microstrip antenna and array", *Int. J. Of AEU*, vol. 77, pp. 76-81, 2017.

[10] J. S. Sun and C. H. Wu, "A broadband circularly polarised antenna of square ring patch for UHF RFID reader application", *Int. J. Of AEU*, vol. 85, pp. 84-90, 2018.

[11] Nasimuddin, Z.N.Chen, and X.Qing, "Asymmetric-circular shaped slotted microstrip antennas for circular polarization and RFID applications," *IEEE Trans. Antennas Propag.*, vol. 58, no. 12, pp. 3821–3828, Dec. 2010.

[12] P. C. Sharma and K. C. Gupta, "Analysis and optimized design of single feed circularly polarized microstrip antennas," *IEEE Trans. Antennas Propag.*, vol. 29, pp. 949–955, 1983.

[13] Nasimuddin, Z. N. Chen, and X. Qing, "A compact circularly polarized cross-shaped slotted microstrip antenna," *IEEE Trans. Antennas Propag.*, vol. 60, no. 3, pp. 1584–1588, March 2012.

[14] A. K. Gautam, A. Kunwar, and B. K. Kanaujia, "Circularly polarized arrowhead-shape slotted microstrip antenna," *IEEE Antennas Wireless Propag. Lett.*, vol. 13, 2014.

[15] Y.-F. Lin, Y.-K. Wang, H.-M. Chen, and Z.-Z. Yang, "Circularly polarized crossed dipole antenna with phase delay lines for RFID handheld reader," *IEEE Trans. Antennas Propag.*, vol. 60, no. 3, pp. 1221–1227, March 2012.

[16] A. Farswan, A.K. Gautam,B. K. Kanaujia, K. Rambabu, "Design of Koch fractal circularly polarized antenna for handheld UHF RFID reader applications," *IEEE Trans. Antennas Propag.*, vol.64, no. 2, pp.771-775, Feb.2016.

[17] V.V.Reddy and N.V.S.N.Sarma,"Triband circularly polarized Koch fractal boundary microstrip antenna," *IEEE Antennas Wireless Propag. Lett.*, vol. 13, 2014.

[18] Hong-Qi Cheng, Li-Bin Tian, Bin-Jie Hu, "Compact Circularly Polarized Square Microstrip Fractal Antenna with Symmetrical T-slits", *in International Conf. on Wireless Communications, Network and Mobile Computing*, pp. 613-616, Sept. 2007.

[19] IE3D Version 14.0. Fremont, CA, Zeland Software Inc., Oct. 2007.

[20] I. K. Kim, J. G. Yook, and H. K. Park, "Fractal-shape small size microstrip patch antenna", *Microw. Opt. Technol. Lett.*, vol. 34, no. 1, pp. 15-17, Jul. 2002.

[21] Mahatthanajatuphat,C. and P.Akkaraekthalin, "An NP generator model for Minkowski fractal antenna," *Proceeding of the 3rd ECTI-CON*, vol. 2, pp.749–752, 2006.

[22] Shashi Kant Pandey, G. P. Pandey, and P. M. Sarun, "Fractal based triple band high gain monopole antenna," *Frequentz*, vol. 71 (11-12), pp. 531-537, Jan. 2017.

[23] N. B. Jin, M.Y. Fan, and X. X. Zhang, "L-band circular polarization microstrip antenna based on the narrow-slot fractal method", in *IEEE AP-S. Int. Symp. Dig.*, vol. 4, pp. 258-261, Jun. 2003.